Volume 1 | Number 1 | Jan 2013 | Pages 1–100

Journal of
Materials Chemistry A

Materials for energy and sustainability
www.rsc.org/materialsA

Li+

e–

e–

Li+

Li+

Li+

ROYAL SOCIETY
OF CHEMISTRY

ROYAL SOCIETY
OF **CHEMISTRY**

www.rsc.org/materialsA

Journal of Materials Chemistry A

Dynamic Article Links▶

COMMUNICATION

Preparation of hollow Co_9S_8 nanoneedle arrays as effective counter electrodes for quantum dot-sensitized solar cells

Chang Chen,[#a] Meidan Ye,[#b] Nan Zhang,[a] Xiaoru Wen,[a] Dajiang Zheng,[a] Changjian Lin[*ab]

Hollow Co_9S_8 nanoneedle arrays directly grown on fluorine-doped tin oxide (FTO) transparent conducting substrates were successfully prepared by a simple sacrificial template method. Performance of the CdS/CdSe quantum dot-sensitized solar cells (QDSCs) employing such Co_9S_8 counter electrodes was remarkably improved as compared to that using the conventional Pt counter electrodes, primarily due to their higher electrocatalytic activity in the reduction of polysulfide electrolyte.

10 One-dimensional (1D) nanomaterials (e.g., nanorods, nanowires) with large surface area, direct electrical pathway and possible quantum effect show excellent application prospect in nanoscale electronic, photonic, electrochemical devices,[1-7] for example, 1D nanoarray materials (e.g., TiO_2 nanorod/nanotube
15 arrays and ZnO nanorod arrays) have been widely applied to the photoelectrochemical devices.[5-8] On the other hand, metal sulphides (e.g., cobalt sulphides, nickel sulphides, and lead sulphide) are the promising electrocatalyst materials and have been extensively utilized in many fields in recent years.[7, 9-14]
20 Especially, since dye/quantum dot-sensitized solar cells (DSCs/QDSCs) have attracted tremendous attention of the researchers, metal sulphides as the counter electrode materials in these DSC/QDSC devices have come into large investigation.[7, 10-12, 15-21] It is well-known that Pt is expensive[7, 22] and a poor
25 electrocatalyst for the reduction of polysulfide electrolyte used in QDSCs,[22] which strongly hold back its application in DSCs/QDSCs. In this regard, many studies have been conducted on the exploitation of alternative electrocatalyst materials as the effective counter electrodes in DSCs/QDSCs, and metal sulphides
30 have been verified the promising counter electrode materials for DSCs and QDSCs.[6, 7, 9, 10, 16, 23-28] Generally, many metal sulphide counter electrodes were prepared by doctor blading on conducting substrates which resulted in poor binding force between the materials and the substrates, and thus weakened the
35 stability of the counter electrodes. Significantly, 1D metal sulphide nanoarray materials directly grown on conductive substrates would avoid this problem and then perform as one of the best candidates of counter electrodes to boost performance of the resulting DSCs and QDSCs. However, to date, ordered metal
40 sulphide nanostructures haven't been studied sufficiently and it is still a great challenge to grow 1D metal sulphide nanoarrays on conductive substrates.

Herein, we report a new method to directly grow Co_9S_8 hollow nanoneedle array films on fluorine-doped tin oxide (FTO)
45 transparent conductive substrates. Such Co_9S_8 hollow nanoneedle array films exhibited large surface area and strong binding force to the FTO substrates. Moreover, they showed higher electrocatalytic ability in the reduction of polysulfide electrolyte, and consequently improved performance of the QDSCs organized
50 by using these Co_9S_8 hollow nanoneedle array based counter electrodes as compared to that using the traditional Pt counter electrode. Furthermore, annealing these Co_9S_8 hollow nanoneedle array films could further enhance the power conversion efficiency of QDSCs.

55 The strategy of preparing Co_9S_8 hollow nanoneedle arrays is shown in Fig. 1. Briefly, two steps were included in this template-assisted method: (1) grow one-dimensional template material $(Co(CO_3)_{0.35}Cl_{0.20}(OH)_{1.10} \cdot 1.74H_2O)$ on FTO substrate by chemical bath deposition in the mixed solution of urea and cobalt
60 chloride; (2) Convert the template materials into the target materials (Co_9S_8) by hydrothermal treatment in sodium sulphide solution. Fig. 2E shows the prepared $Co(CO_3)_{0.35}Cl_{0.20}(OH)_{1.10} \cdot 1.74H_2O$ template. Nanoneedles were grown uniformly on the FTO substrate with a diameter of around
65 200 nm and length of several micrometers (Fig. 2E), which were solid and single crystal proven by SAED pattern (inset in Fig. 2A) and HRTEM (Fig. 2B). After hydrothermally treated in 10 mM Na_2S aqueous solution under 180 ℃ for 10 h, the solid nanoneedle templates were converted into hollow nanoneedles
70 which was confirmed by TEM image (Fig. 2C). The corresponding cross-sectional view indicated that such nanoneedle was hexagon (inset in Fig. 2C) and its phase was Co_9S_8 which was confirmed by XRD pattern (Fig. 3A, JCPDS. NO. 03-065-3322, Pa-3, a = b = c = 0.5535 nm).The surface of
75 nanoneedles became rough but the needle-like structure changed little after the hydrothermal conversion (Fig. 2F).
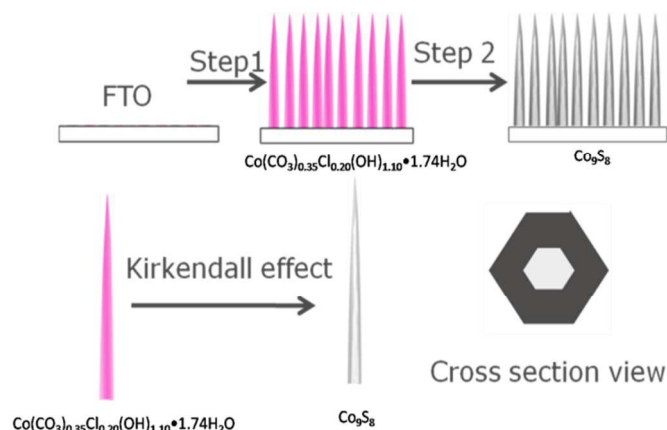
Fig. 1 Schematic diagram of preparing the Co_9S_8 nanoneedle arrays on FTO substrates.
80
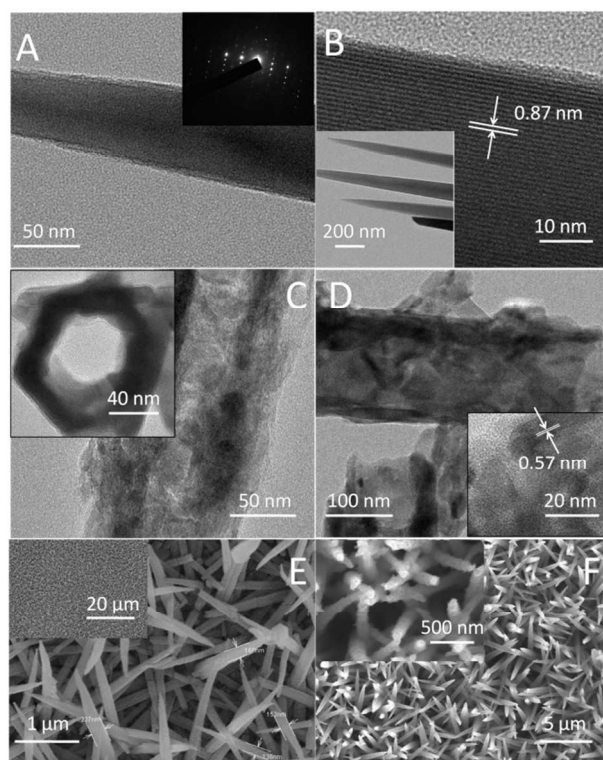
Fig. 2 TEM and SEM images of $Co(CO_3)_{0.35}Cl_{0.20}(OH)_{1.10} \cdot 1.74H_2O$ templates (A, B and E), inset of A is the corresponding SAED pattern. TEM images of Co_9S_8 prepared by hydrothermally treating $Co(CO_3)_{0.35}Cl_{0.20}(OH)_{1.10} \cdot 1.74H_2O$ templates for 10 h (C) and annealed it at 400 °C for 30 min in N_2 gas (D). SEM images of Co_9S_8 prepared by hydrothermally treating $Co(CO_3)_{0.35}Cl_{0.20}(OH)_{1.10} \cdot 1.74H_2O$ templates for 10 h (F).

Fig. 3 XRD patterns of (A) $Co(CO_3)_{0.35}Cl_{0.20}(OH)_{1.10} \cdot 1.74H_2O$ prepared by hydrothermally treating FTO substrates in Na_2S aqueous solution for different time. Diffraction peaks of $Co(CO_3)_{0.35}Cl_{0.20}(OH)_{1.10} \cdot 1.74H_2O$ were labelled by Red start (*); (B) the pristine Co_9S_8 (Co_9S_8) and Co_9S_8 annealed in N_2 at 400 °C for 30 min (Co_9S_8-an). Diffraction peaks of Co_9S_8 were labelled by red '#'.

XRD pattern (Fig. 3A) showed that with the increasing of hydrothermal reaction time, the intensity of diffraction peaks of the $Co(CO_3)_{0.35}Cl_{0.20}(OH)_{1.10} \cdot 1.74H_2O$ templates decreased and almost disappeared when the reaction time was prolong to 7 h, suggesting that the $Co(CO_3)_{0.35}Cl_{0.20}(OH)_{1.10} \cdot 1.74H_2O$ templates were already completely consumed after 7 h. The conversion from solid $Co(CO_3)_{0.35}Cl_{0.20}(OH)_{1.10} \cdot 1.74H_2O$ nanoneedle templates to hollow Co_9S_8 nanoneedles by hydrothermal treatment can be explained by the Kirkendall effect.[29] Briefly, at the early stage under high temperature, Co_9S_8 was firstly formed on the surface of the nanoneedle templates; later on the cobalt ions at the center were diffused to the surface of the nanoneedle templates and then reacted with sulfur ions to form cobalt sulphide. As reaction time increased, the cobalt ions were exhausted at the center of the nanoneedle templates and other species, such as CO_3^{2-} and Cl^-, were dissolved in the hydrothermal solution, resulting in the hollow nanoneedles. Furthermore, annealing effect on the crystalline degree of the Co_9S_8 films was conducted as well. After annealing (Fig. 2D) treatment in N_2 atmosphere at 400°C for 30 min, the crystalline degree of Co_9S_8 nanoneedles was improved dramatically compared with the pristine sample (Fig. 2C), which was also confirmed by some new and strengthened diffraction peaks of Co_9S_8 phase in XRD patterns (Fig. 3B). However, the binding force between Co_9S_8 films and FTO substrates became weak and very easy to shed after hydrothermal conversion. And the $TiCl_4$ pre-treatment of FTO substrates before growing templates (see experimental section) could enhance the binding force between the Co_9S_8 films and the FTO substrates.

Electrochemical catalytic ability of the Co_9S_8 films on FTO substrates was studied by Tafel polarization curves and electrochemical impedance spectra (EIS). In Tafel polarization curves, the exchange current density (J_0) is directly related to the catalyst ability of the electrodes, which can be estimated from the extrapolated intercepts of the anodic and cathodic branches of the corresponding Tafel polarization curves.[30] As showed in Fig. 4A, Tafel polarization curves of the un-annealed Co_9S_8 and annealed Co_9S_8 electrodes (Co_9S_8-an) were both higher than that of Pt electrode with around two order of magnitude, implying that the J_0 values of the Co_9S_8 and Co_9S_8-an electrode were higher than that of Pt electrode with nearly an order of magnitude, and then the electrocatalytic ability in reduction of polysulfide electrolyte for Co_9S_8 and Co_9S_8-an electrode was superior. It was found that the Tafel polarization curve of Co_9S_8-an electrode was slightly higher than that of Co_9S_8 electrode, suggesting the better electrocatalytic ability of the Co_9S_8-an electrode, which was ascribed to the higher crystallinity and thus better electron transfer pathway in the annealed Co_9S_8 nanoneedle. The same conclusion was obtained from the EIS test (Fig. 4B). Large semicircle of the curves accounts for large electron transfer resistance (R_{ct}) at the electrode/electrolyte interface while small semicircle relates to the small R_{ct} (fitting values of R_{ct} by ZSimpWin software with the equivalent circuit in Fig. 4B were shown in Table 1).[30] Co_9S_8-an got the smallest semicircle and thus had the best electrocatalytic ability in the three electrodes.
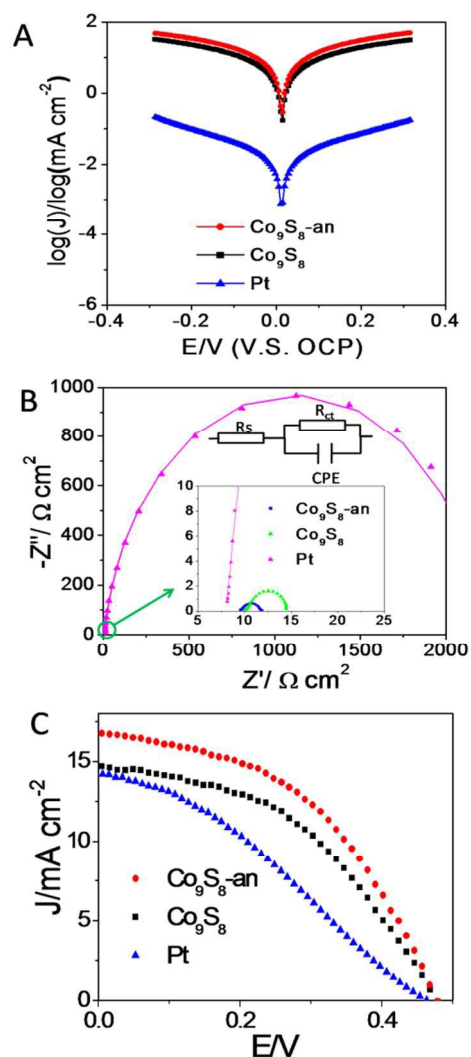
Fig. 4 (A) Tafel polarization curves of different counter electrodes, which were tested by using symmetrical cells with an active area of 0.21 cm^{-2}. (B) Electrochemical impedance spectra (EIS) of the QDSCs based on the
5 three different counter electrodes. The dot lines and solid lines were measured curves and their corresponding fitted curves calculated by the ZSimpWin software according to the given circuit in the top inset, respectively, and the button inset shows the enlarged Nyquist plots marked with green cycle. (C) J-V curves of the QDSCs assembled by
10 different counter electrodes, and the cell active area is 0.21 cm^{-2}.

Table 1. Photovoltaic parameters of the QDSCs based on different counter electrodes.

Counter electrode	V_{oc} (V)	J_{sc} (mA cm^{-2})	FF (%)	Eff (%)	R_{ct} (Ω cm^{-2})
Pt	0.47	14.23	32.00	2.12	2213
Co$_9$S$_8$	0.48	14.72	44.04	3.13	4.59
Co$_9$S$_8$-an	0.48	16.80	46.18	3.72	2.29

Photocurrent density-voltage (J-V) curves of the QDSCs
15 based on Co$_9$S$_8$, Co$_9$S$_8$-an and Pt counter electrodes (CEs) were obtained under simulated sunlight. As showed in Fig. 4C and Table 1, the open-circuit voltage (V_{oc}) of the QDSCs was not affected by the CEs. The QDSCs with Co$_9$S$_8$ CEs showed a short circuit current density (J_{sc}) of 14.72 mA cm^{-2}, which was a little
20 higher than that with Pt CEs (14.23 mA cm^{-2}). But the fill factor

(FF) of QDSCs with Co$_9$S$_8$ CEs (44.04%) was much higher than that of Pt CEs (32.00%), and consequently the efficiency of QDSCs with Co$_9$S$_8$ CEs (3.13%) was much higher than that with Pt CEs (2.12%), which was ascribed to the higher electrocatalytic
25 ability of Co$_9$S$_8$ in reduction of polysulfide electrolyte used in QDSCs (Fig. 4A and 4B). Furthermore, the QDSCs with Co$_9$S$_8$-an CEs showed a higher J_{sc} (16.80 mA cm^{-2}) than that with Co$_9$S$_8$ CEs and thus obtained a higher power conversion efficiency (3.72%), which was in line with the electrocatalytic ability
30 discussed in Tafel polarization and EIS tests above.

Conclusion

In conclusion, a method of preparing Co$_9$S$_8$ hollow nanoneedle array films directly grown on FTO substrates was put
35 forward. The TiCl$_4$ pre-treatment of FTO substrates enhanced the binding force between the Co$_9$S$_8$ films and FTO substrates. We got an improved efficiency of 3.72% from QDSCs with this Co$_9$S$_8$ CEs and boosted the efficiency of traditional QDSCs with Pt CEs by 75%. What is more important, our method can be
40 applied to prepare other metal sulphides or even metal selenides grown on FTO substrates.

Notes and references

^{a}*State Key Laboratory of Physical Chemistry of Solid Surfaces, and Department of Chemistry, College of Chemistry and Chemical Engineering, Xiamen University, Xiamen 361005, China*
50 ^{b}*Research Institute for Soft Matter and Biomimetics, School of Physics and Mechanical & Electrical Engineering, Xiamen University, Xiamen, 361005, China*

$^\#$*These authors contribute to this work equally.*

55 **To whom correspondence should be addressed. Email: cjlin@xmu.edu.cn*

† Electronic Supplementary Information (ESI) available: Experimental details. See DOI: 10.1039/c000000x/

60 1.   Z. Wang, L. Pan, H. Hu and S. Zhao, *CrystEngComm*, 2010, **12**, 1899-1904.
2.   P. F. Yin, L. L. Sun, Y. L. Gao and S. Y. Wang, *Bull. Mater. Sci.* , 2008, **31**, 593-596.
3.   S. Q. Wang, G. H. Li, Y. P. He, H. Y. Yin, Z. D. Xu and B. S.
65   Zou, *Mater. Lett.* , 2006, **60**, 815-819.
4.   M. Q. Lv, D. J. Zheng, M. D. Ye, J. Xiao, W. X. Guo, Y. K. Lai, L. Sun, C. J. Lin and J. Zuo, *Energy Environ. Sci.* , 2013, **6**, 1615-1622.
5.   M. Lv, D. Zheng, M. Ye, L. Sun, J. Xiao, W. Guo and C. Lin,
70   *Nanoscale*, 2012, **4**, 5872-5879.
6.   M. D. Ye, X. K. Xin, C. J. Lin and Z. Q. Lin, *Nano Lett.* , 2011, **11**, 3214-3220.
7.   C. W. Kung, H. W. Chen, C. Y. Lin, K. C. Huang, R. Vittal and K. C. Ho, *ACS Nano*, 2012, **6**, 7016-7025.
75 8.   Y. Zhang, L. Ge, M. Li, M. Yan, S. Ge, J. Yu, X. Song and B. Cao, *Chem. Commun. (Cambridge, U. K.)*, 2014, **50**, 1417-1419.
9.   P. Sudhagar, S. Nagarajan, Y. G. Lee, D. Song, T. Son, W. Cho, M. Heo, K. Lee, J. Won and Y. S. Kang, *ACS Appl.*
80   *Mater. Interfaces* 2011, **3**, 1838-1843.

10. M. K. Wang, A. M. Anghel, B. Marsan, N. L. C. Ha, N. Pootrakulchote, S. M. Zakeeruddin and M. Gratzel, *J. Am. Chem. Soc.* , 2009, **131**, 15976-+.

11. Z. Yang, C.-Y. Chen and H.-T. Chang, *Sol. Energy Mater. Sol. Cells* 2011, **95**, 2867-2873.

12. J. B. Zhang, F. Y. Zhao, G. S. Tang and Y. Lin, *Journal of Solid State Electrochemistry*, 2013, **17**, 2909-2915.

13. M. Yuan, K. W. Kemp, S. M. Thon, J. Y. Kim, K. W. Chou, A. Amassian and E. H. Sargent, *Adv. Mater.* , 2014, **26**, 3513-3519.

14. K. S. Jeong, J. Tang, H. Liu, J. Kim, A. W. Schaefer, K. Kemp, L. Levina, X. Wang, S. Hoogland and R. Debnath, *Acs Nano*, 2011, **6**, 89-99.

15. W. X. Guo, C. Xu, X. Wang, S. H. Wang, C. F. Pan, C. J. Lin and Z. L. Wang, *J. Am. Chem. Soc.* , 2012, **134**, 4437-4441.

16. Y. Shengyuan, A. S. Nair, Z. Peining and S. Ramakrishna, *Mater Lett*, 2012, **76**, 43-46.

17. X. Yu, J. Zhu, F. Liu, J. Wei, L. Hu and S. Dai, *Sci. China: Chem.*, 2013, **56**, 977-981.

18. W. Zhao, X. Zhu, H. Bi, H. Cui, S. Sun and F. Huang, *J. Power Sources* 2013, **242**, 28-32.

19. Z. Zhou, M. Ge, H. Zhang, P. Xu, L. Liu and J. Wei, Nankai University, Peop. Rep. China . 2013, p. 8pp.

20. E. H. Sargent, *Nano Lett.* , 2014.

21. G. H. Kim, B. Walker, H. B. Kim, J. Y. Kim, E. H. Sargent and J. Park, *Adv. Mater.* , 2014, **26**, 3321-3327.

22. Z. S. Yang, C. Y. Chen, C. W. Liu, C. L. Li and H. T. Chang, *Adv Energy Mater*, 2011, **1**, 259-264.

23. B. Wang, J. Park, D. W. Su, C. Y. Wang, H. Ahn and G. X. Wang, *J Mater Chem*, 2012, **22**, 15750-15756.

24. S. S. Kalanur, S. Y. Chae and O. S. Joo, *Electrochim. Acta* 2013, **103**, 91-95.

25. A. Banerjee, K. K. Upadhyay, S. Bhatnagar, M. Tathavadekar, U. Bansode, S. Agarkar and S. B. Ogale, *RSC Adv.*, 2014, **4**, 8289-8294.

26. M. Liu, G. Li and X. Chen, *ACS Appl. Mater. Interfaces* 2014, Ahead of Print.

27. J. Ma, J. Chen, C. Li and L. Wu, Tongji University, Peop. Rep. China . 2014, p. 11pp.

28. L. Wang, Y. Shi, Y. Wang, H. Zhang, H. Zhou, Y. Wei, S. Tao and T. Ma, *Chem. Commun. (Cambridge, U. K.)*, 2014, **50**, 1701-1703.

29. W. Shi, J. Zhu, X. Rui, X. Cao, C. W. Chen, H. Zhang, H. H. Hng and Q. Yan, *ACS Appl. Mater. Interfaces* 2012, **4**, 2999–3006.

30. M. Ye, C. Chen, N. Zhang, X. Wen, W. Guo and C. Lin, *Adv. Energy Mater.*, 2014, 201301564.

Journal of Materials Chemistry A

COMMUNICATION

The table of contents entry

Preparation of hollow Co_9S_8 nanoneedle arrays as effective counter electrodes for quantum dot-sensitized solar cells

Chang Chen,[a] Meidan Ye,[b] Nan Zhang,[a] Xiaoru Wen,[a] Dajiang Zheng,[a] Changjian Lin[*ab]

[a]State Key Laboratory of Physical Chemistry of Solid Surfaces, and Department of Chemistry, College of Chemistry and Chemical Engineering, Xiamen University, Xiamen 361005, China

[b]Research Institute for Soft Matter and Biomimetics, School of Physics and Mechanical & Electrical Engineering, Xiamen University, Xiamen, 361005, China

[*]To whom correspondence should be addressed. Email: cjlin@xmu.edu.cn
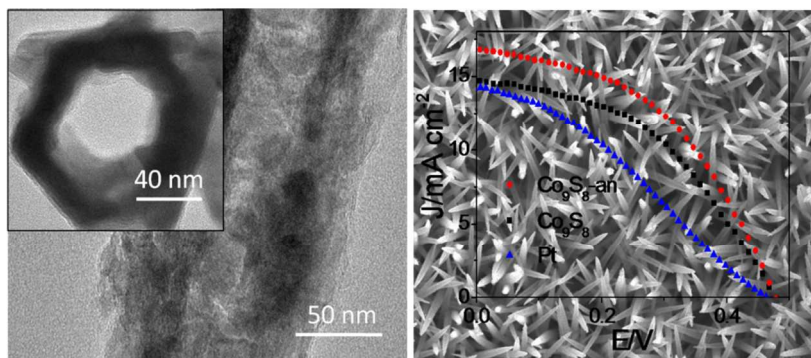
Hollow Co_9S_8 nanoneedle arrays were directly grown on transparent conducting substrates via a simple template-assisted hydrothermal process using $Co(CO_3)_{0.35}Cl_{0.20}(OH)_{1.10} \cdot 1.74H_2O$ nanoneedle array films as templates. Upon calcination post-treatment, the resulting CdS/CdSe QDSCs based on such cobalt sulfide counter electrodes exhibited a high power conversion efficiency of 3.72%.